Characterization and Reactivity of Nanosized Calcium Phosphates Prepared in Anhydrous Ethanol

Pierre Layrolle and Albert Lebugle*

Laboratoire des Matériaux, Physico-chimie des Solides, URA CNRS 445, Ecole Nationale Superieure de Chimie, Institut National Polytechnique de Toulouse, 38 rue des 36 ponts, 31400 Toulouse, France

Received April 7, 1994. Revised Manuscript Received August 8, 1994[⊗]

A new synthesis route of different calcium phosphates, using calcium diethoxide ($Ca(OEt)_2$) and orthophosphoric acid (H_3PO_4) as reagents and anhydrous ethanol as solvent is described. By simple variance of the ratio of reagents from 1/1, 8/6, to 9/6, calcium phosphates of various chemical compositions $Ca_x(HPO_4)_y(PO_4)_z$ are precipitated in the ethanol. The solids which form were characterized by different physicochemical analyses, and their thermal behavior was studied by TGA, DTA, chemical analyses, XRD, IR spectroscopy, specific surface areas, and SEM observations. The series of physicochemical results show that the different solid calcium phosphates are amorphous and nanosized and have large specific surface areas and high reactivities. The thermal crystallization and very active sintering at low temperatures, led to metastable β-$Ca_2P_2O_7$ and α-$Ca_3(PO_4)_2$.

Introduction

Calcium phosphates have numerous industrial applications in very different domains.[1] They are used in the manufacture of fertilizers, in the treatment of liquid waste, in toothpaste and cosmetics, and also in the form of ceramics for the coating of protheses such as bone and dental substitutes.[2,3] The most common form of apatitic calcium phosphate is stoichiometric hydroxyapatite $Ca_{10}(PO_4)_6(OH)_2$, in which many ionic substitutions can occur.[4,5] Apatites are the principal inorganic constituents of the hard tissues in vertebrates (bones and teeth). In these biological tissues, calcium phosphates are often associated with macromolecules such as collagen or proteins.[6] So, they form real mineral–organic composites that give them good mechanical properties. Several authors have shown that the mineral part of these calcified tissues presents a poor crystallinity due to the very divided state of the material as nanocrystals.[7–11] Naturally, the preparation of calcium phosphates of a chemical composition close to that of bone mineral in aqueous media has been thoroughly investigated.[12–17] It has been proposed that the formation of crystalline calcium phosphates is preceded by an amorphous calcium phosphate (ACP). This ACP precipitate in aqueous slurries becomes spontaneously transformed into hydroxyapatite by a process of solution and renucleation. Several authors have established that the presence of nonaqueous solvents in the precipitation solution favors and stabilizes the formation of ACP. Although syntheses in water are widely described in the literature, only few attempts in water–ethanol mixtures have been reported.[18–23] During previous work, we showed that the use of partially aqueous solvents permits the preparation of compounds which are not obtained in pure water. For example, the coprecipitation of a phosphate grafted to an organic molecule and an apatitic calcium phosphate mineral.[24–27] This allowed us to obtain new hybrid mineral–organic materials.[28,29]

For these reasons, it is of interest to prepare these calcium phosphates in a nonaqueous media. The results of the first synthesis of mineral calcium phosphates in a pure organic solvent are set out here. Different compounds were precipitated in ethanol starting from

[⊗] Abstract published in *Advance ACS Abstracts,* October 1, 1994.

(1) Kanazawa, T. *Inorganic phosphate materials*; Materials science monographs, 52 Kodansha Tokyo, and Elsevier Science publishers B.V.: Amsterdam, 1989; p 15.
(2) Legeros, R. Z. *Calcium phosphates in oral biology and medecine*; Karger: Basel, 1991.
(3) De Groot, K. *Ceramics in Surgery*; Vincezini, P., Ed.; Elsevier: Amsterdam, 1983.
(4) Legeros, R. Z. *Prog. Cryst. Growth Charc.* **1981**, *4*, 1.
(5) Colloque Internationnal CNRS, *Physico-chimie et Cristallographie des apatites d'interet biologique*, Paris, 1975.
(6) Glimcher, M. J. *Philos. Trans. R. Soc. London* **1984**, *B304*, 479.
(7) Marshall, R.; Urist, M. D. *Fundamental and clinical bone physiology*; J. B. Lippincott: Philadelphia, 1980; p 7.
(8) Eanes, E. D.; Termine, J. D.; Posner, A. S. *Clin. Orthop. Rel. Res.* **1967**, *53*, 223–35.
(9) Posner, A. S. *Physiol. Rev.* **1969**, *49*, 760.
(10) Betts, F.; Posner, A. S. *Trans. Am. Cryst. Assoc.* **1974**, *10*, 73.
(11) Posner, A. S.; Betts, F. *Acc. Chem. Res.* **1975**, *8*, 277.
(12) Eanes, E. D.; Gillensen, I. H.; Posner, A. S. *Nature* **1965**, *208*, 365.
(13) Termine, J. D.; Peckauskas, R. A.; Posner, A. S. *Arch. Biochem. Biophys.* **1970**, *140*, 318.
(14) Blumenthal, N. C.; Posner, A. S.; Holmes, J. M. *Mater. Res. Bull.* **1972**, *7*, 1181.
(15) Boskey, A. L.; Posner, A. S.*J. Phys. Chem.* **1973**, *77*, 2313.
(16) Posner, A. S.; Betts, F. *Acc. Chem. Res.* **1975**, 8, 273.
(17) Heughebaert, J. C.; Montel, G. *Calcif. Tissue Int.* **1982**, *34*, 103.
(18) Zahidi, E.; Lebugle, A.; Bonel, G. *Bull. Soc. Chim. Fr.* **1985**, *4*, 523.
(19) Lebugle, A.; Zahidi, E.; Bonel, G. *Reactivity Solids* **1986**, *2*, 151.
(20) Julia, A.; Lebugle, A. *J. Solid State Chem.* **1990**, *84*, 342.
(21) Joost Larsen, M.; Thorsen, A.; Jensen, S. J. *Calcif. Tissue Int.* **1985**, *37*, 189.
(22) Lerner, E.; Azoury, R.; Sarig, S. *J. Cryst. Growth* **1989**, *97*, 725.
(23) Thung, M. S.; O'Farrell, T. J. *J. Mol. Liquids* **1993**, *56*, 237.
(24) Lebugle, A.; Zahidi, E.; Bonel, G. *Innov. Tech. Biol. Med.* **1982**, *3*, 626.
(25) Montel, G.; Bonel, G.; Lebugle, A.; Subirade, M. *C. R. Acad. Sci. Paris* **1989**, *309 (II)*, 1155.
(26) Subirade, M.; Lebugle, A. *Ann. Chim. Fr.* **1991**, *16*, 89.
(27) Subirade, M.; Lebugle, A. *Ann. Chim. Fr.* **1993**, *18*, 183.
(28) Delpech, V.; Lebugle, A. *Clin. Mater.* **1990**, *5*, 209.
(29) Dandurand, J.; Delpech, V.; Lebugle, A.; Lamure, A.; Lacabanne, C. *J. Biomed. Mater. Res.* **1990**, *24*, 1377.

0897-4756/94/2806-1996$04.50/0 © 1994 American Chemical Society

Table 1. Chemical Microanalysis of Calcium Diethoxide, $Ca(OEt)_2$

elements	exp wt obtained (%)	theor wt determined in $Ca(OEt)_2$ (%)
Ca[a]	30.3	30.8
C[b]	36.4	36.9
H[b]	7.5	7.7
O[c]	25.8	24.6

[a] Calcium was assayed by the complexometric method described in the Experimental Section. The value was the average of four determinations. [b] Based on the microanalyses of C and H. [c] Oxygen content was calculated by difference to 100%.

$Ca(OEt)_2$ and H_3PO_4. The solids which formed were characterized by different physicochemical analyses, and their thermal behavior was studied.

Experimental Section

Materials. All the experiments were performed in an atmosphere of dry argon with vacuum manifolds for air-sensitive products. Conventional glassware was used. Calcium metal shavings (99 %, Aldrich) and phosphoric acid crystals (98+ %, Aldrich) were used as received. Anhydrous ethanol (Prolabo) was dried over 4 Å molecular sieves and freshly distilled before use.

Preparation of the Calcium Diethoxide Solution. The calcium diethoxide $Ca(OEt)_2$ was prepared by reacting the appropriate amounts of calcium metal with anhydrous ethanol with generation of hydrogen gas:

$$Ca + 2EtOH \rightarrow Ca(OEt)_2 + H_2\uparrow \quad (1)$$

Several precautions were taken during the synthesis of $Ca(OEt)_2$. The most important was to exclude moisture and air before, during, and after the reaction, because $Ca(OEt)_2$ is very moisture- and air-sensitive. The glassware, calcium metal, and ethanol used were dried and a dry atmosphere (argon) was essential. These measures were to prevent the precipitation of the hydrolyzed product, i.e., $Ca(OH)_2$ and the carbonate salt, i.e., $CaCO_3$. The appropriate amount of calcium metal shavings and 50 mL of dry ethanol were put in a 100-mL three-neck round bottom flask with a heater–magnetic stirrer and a condenser under argon gas. The dispersion was refluxed for 4 h until all the metallic calcium disappeared. The pH of the clear solution obtained, named **SOL A**, reached 13.3. For the chemical analysis of $Ca(OEt)_2$, **SOL A** was cooled to room temperature and concentrated under reduced pressure until white crystals precipited. The fine white powder was dried under vacuum to remove the solvent. $Ca(OEt)_2$ was obtained quantitavely and pure as reported in Table 1.

Preparation of the Orthophosphoric Acid Solution. The solution of orthophosphoric acid named **SOL B** was prepared as follows. The appropriate amount of anhydrous H_3PO_4 crystals were dissolved by stirring under argon gas in 50 mL of dried ethanol at room temperature in a 250-mL three-neck round-bottom flask. Then, this solution was either cooled to 5 °C in an ice bath or heated to 80 °C with a hot plate and refluxed with a condenser. The temperature was monitored with a thermocouple plunged into **SOL B**.

Synthesis of Calcium Phosphates. The quantity of reagents in the two solutions is indicated in Table 2. The different Ca/P molar ratios chosen agreed with the well-known compounds of the phase diagram of $CaO–P_2O_5–H_2O$. So, the ratios 1.00, 1.33, and 1.50 correspond respectively to dicalcium phosphate (DCP) $CaHPO_4$, octacalcium phosphate (OCP, $Ca_8H_2(PO_4)_4{\cdot}5H_2O$ described by Brown et al.,[30] and tricalcium phosphate (TCP) $Ca_3(PO_4)_2$.

SOL A was added quickly through a nozzle to vigourously stirred **SOL B**, a gelatinous precipitate of calcium phosphate was obtained. Then, it was stirred for 10 min at the desired temperature and centrifuged for 15 min at 4000 rpm in two centrifuge tubes. The surpernatant solution was removed. The solid was dried under vacuum at room temperature overnight. Then, the fine white powder was crushed in an agate mortar and stored in a Schlenck container under argon gas at −20 °C in a refrigerator to prevent hydrolysis and crystallization.

Table 2. Synthesis Conditions of Calcium Phosphates: Ca/P Liquid Molar Ratio, Quantities of Reagents, and Temperature of Reaction

samples	Ca/P liquid (molar ratio)	SOL A[a] g	SOL A[a] mmole	SOL B[a] g	SOL B[a] mmole	reaction temp (°C)
A	1.00	0.806	20.1	1.957	20.0	5
B	1.00	0.844	22.0	2.070	21.1	80
C	1.34	1.028	25.7	1.880	19.2	80
D	1.52	1.172	29.3	1.891	19.3	80

[a] +50 mL of EtOH.

Analytical Techniques. Thermogravimetric and differential thermal analyses (TGA, DTA) were executed on a Setaram TG-DTA 92 thermobalance in the temperature range 20–1000 °C at heating rates of 10 °C min^{-1} under a U-grade helium atmosphere (flow 1 L h^{-1}) with about 20 mg of the dried sample in cylindrical platinum crucibles.

The final products were chemically analysed as follows: 100 mg of the dried powder was dissolved in 5 mL of perchloric acid (2 M) in a 100-mL volumetric flask. Calcium was titrated by a complexometric method using EDTA disodium salt in the presence of zinc chloride and with Eriochrome black T as an indicator.[31] The relative error on calcium determination was 1%. The orthophosphate content was determined by the vanadomolybdate spectrophotometric method[32] at 460 nm using a Beckman Model 24 spectrophotometer with a relative error of 1%. The instrument was calibrated using standard solutions of KH_2PO_4. The amount of pyrophosphate ion was determined after calcination of the sample in a platinum crucible at 700 ± 10 °C in a tubular furnace for 10 h. Hydrogen phosphate ions reacted together at high temperature to form pyrophosphate ions according to the reaction

$$2HPO_4^{2-} \rightarrow P_2O_7^{4-} + H_2O\uparrow \quad (2)$$

Then, the phosphate was assayed by the spectrophotometric method before and after hydrolysis of the P–O–P bond in perchloric acid (6 M) at 100 °C for 1 h.[33] Absorbances were measured in the optical density range 0.05–0.6. The calcium-to-phosphorous atomic ratios Ca/P were found to correspond to the values expected from the starting materials to within ±0.01.

Carbon and hydrogen microanalyses of solids were obtained with a Carlo-Erba Model 1106 elemental analyzer. The relative errors on the determination of these elements were respectively 0.3 and 0.1%.

Thermal Treatment. The thermal behavior of the different calcium phosphates prepared in ethanol and vacuum dried were examined in the range 20–900 °C by X-ray diffraction, IR spectroscopy, chemical analysis and scanning electron microscopy. The samples were placed in a platinum boat and then into a silica laboratory tube, in which helium was circulated (flow 1 L h^{-1}). Samples were heated progressively from room to the desired temperature at heating rates of 10 °C min^{-1}. After a stage of 10 h at the desired temperature, solids were rapidly cooled to 20 °C and studied by the different physico-chemical analyses.

X-ray Diffraction. XRD patterns of the solids were recorded at room temperature for 1 h, with Co $K\alpha_1$ radiation (λ = 1.788 92 Å) using an INEL CPS 120 diffractometer operating at 45 kV and 28 mA. For the precise determination of d_{hkl} values or 2θ angles, α-Al_2O_3 (30 wt %) was used as an

(30) Brown, W. E.; Smith, J. P.; Lehr, J. F.; Frazier, A. W. *Nature* **1962**, *196*, 1048.

(31) Charlot, G. *Les Méthodes de la Chimie Analytique, Analyse Quantitative et Minérale*, 5th ed.; Masson and Cie: Paris, 1966; p 657.
(32) Gee, A.; Deitz, V. R. *Anal. Chem.* **1953**, *25*, 1320.
(33) Gee, A.; Deitz, V. R. *J. Am. Chem. Soc.* **1955**, *77*, 2961.

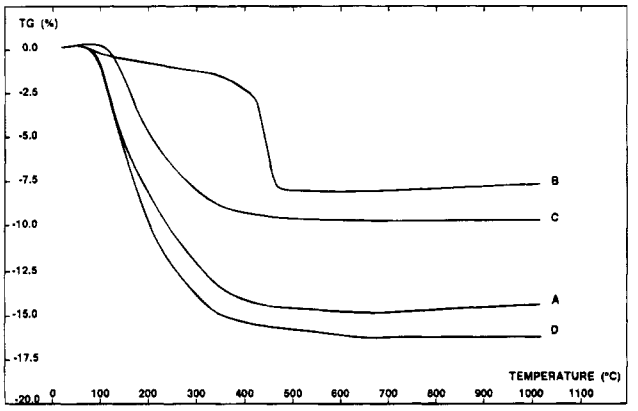

Figure 1. TGA curves of the different dried powders of calcium orthophosphates prepared in anhydrous ethanol with various Ca/P liquid ratios and reaction temperatures. (**A**) $[Ca/P]_L = 1.00$, $T_R = 5$ °C; (**B**) $[Ca/P]_L = 1.00$, $T_R = 80$ °C; (**C**) $[Ca/P]_L = 1.34$, $T_R = 80$ °C; (**D**) $[Ca/P]_L = 1.51$ $T_R = 80$ °C.

internal standard (JSPDS 10-173). For comparaison all the patterns were reported with the same scale.

Infrared Spectroscopy. Infrared spectra (IR) were obtained over the 4000–400-cm^{-1} region on a Perkin-Elmer FT-IR 1600 spectrometer using KBr pellets: about 1 mg of the sample was mixed and crushed in an agate mortar with 300 mg of potassium bromide (Prolabo, spectroscopic grade). Transparent pellets were obtained under vacuum (~1 Torr) and pressed at 14 tons cm^{-2}.

Specific Surface Area Determinations. The specific surface areas were determined by the single-point Brunauer–Emmett–Teller (BET) method using nitrogen adsorption-desorption with a Quantasorb II Quantachrome, Greenvale, NY, apparatus. About 30 mg of the sample was weighed in a special tube, and it was placed in an oven at 100 °C for 1 h. Then, the powder was degased with a helium/nitrogen mixture for 1 h. The precision of the specific surface area measurements was ±5%.

Scanning Electron Micrographs. Particle sizes were measured using a JEOL JSM-6400 scanning electron microscope. For SEM observations, the powder was ultrasonically dispersed for 5 min in ethanol. Then, the suspension was deposited on a carbon support , dried under vacuum, and metallized with Ag for 1–2 min.

Results

The different calcium phosphates were prepared using $Ca(OEt)_2$ and H_3PO_4 as initial compounds in pure ethanol, according to the experimental procedure described above, and the resulting solids were characterized.

Thermal Analyses. Thermogravimetric (TGA) and differential thermal analyses (DTA) of the corresponding calcium phosphate precipitates **A**–**D** after drying in vacuo are presented in Figures 1 and 2.

The TGA curves of the three solids **A**, **C**, and **D** in Figure 1 show a single and continuous weight loss of respectively 14.7, 9.7, and 15.2%. These weight losses, which occurred in the temperature range 100–500 °C, can be attributed to the evaporation and desorption of ethanol and also, in certain compounds, to the condensation of HPO_4^{2-} ions according to reaction 2. Two weight losses can be seen in the TGA curve of sample **B**. The first spreads out between 100 and 315 °C with a weight loss of 1% which can be attributed to the removal of the residual solvent. The second equal to 6.7 wt % is sudden, occurring between 375 and 475 °C.

The DTA curves of the precipitates are shown in Figure 2. As before, the evolution of sample **B** is

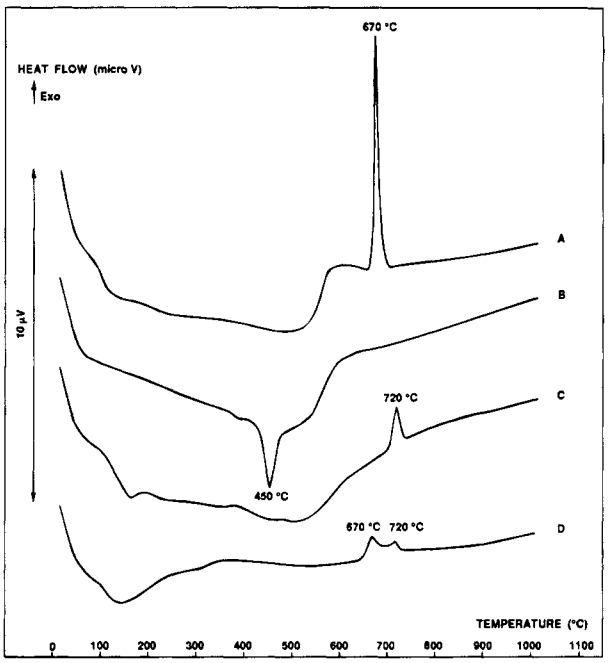

Figure 2. DTA profiles of the different samples prepared in various conditions. (**A**) $[Ca/P]_L = 1.00$, $T_R = 5$ °C; (**B**) 1.00, 80 °C; (**C**) 1.34, 80 °C; (**D**) 1.51, 80 °C.

Table 3. Chemical Compositions of Dried Calcium Phosphates Precipitates Prepared in Ethanol

samples	Ca/P liquid (molar ratio); temp (°C)	chem analyses (wt %) % Ca[a]	% PO_4[b]	% EtOH[c]	total	Ca/P solid (atomic ratio)
A	1.00; 5	26.5	61.8	11.2	99.5[d]	1.02
B	1.00; 80	29.3	67.9	1.0	98.2[d]	1.02
C	1.34; 80	32.4	58.0	9.0	99.4[d]	1.33
D	1.52; 80	33.0	51.9	15.2	100.1	1.51

[a] The calcium was determined by the complexometric method. [b] The orthophosphate content was determined by the spectrophotometric method. [c] The weight percentage of ethanol was calculated from the weight loss recorded in TGA after taking the deshydration of HPO_4^{2-} ions into account. [d] The difference from 100% is due to the hydrogen content of HPO_4^{2-}.

different from the others. A wide endothermic effect at 450 °C is observed in the DTA curve which corresponds to the second weight loss in the TGA. This negative enthalpy is associated to the dehydratation of HPO_4^{2-} ions into pyrophosphate ions according to reaction 2. For samples **A**, **C**, and **D**, the DTA curves indicate an endothermic drift between 100 and 500 °C with a maximum at about 150 °C. This endothermic effect corresponds to the continuous decrease of the weight loss observed in TGA. Then, exothermic signals are observed between 650 and 750 °C due to sample crystallization. The DTA of solid **A** indicates a strong exothermic effect at 670 °C. Sample **C** shows a much weaker exothermic peak at 720 °C. The DTA curve of sample **D** displays two close exothermic peaks at 670 and 720 °C.

Chemical Characterization. The results of the chemical analyses of the different calcium phosphate precipitates prepared in ethanol, centrifuged, and dried under vacuum are gathered in Table 3. The calcium to phosphorus atomic ratios in the solids are close to the molar Ca/P ratios in solution. The quantity of ethanol in the samples was calculated with the weight loss recorded in TGA, after taking account of the weight loss due to the transformation of HPO_4^{2-} into $P_2O_7^{4-}$.

Table 4. Chemical Composition and Formulas of Calcium Phosphates Heated to 700 °C in Helium for 10 h

	chemical analysis						
	Ca^a		PO_4^b		$P_2O_7^c$		
samples	mole	wt %	mole	wt %	mole	wt %	found formula at 700 °C
A	0.78	31.2	≤0.01	≤1	0.39	67.9	$Ca_2(P_2O_7)_{0.99}$
B	0.79	31.6	≤0.01	≤1	0.39	67.8	$Ca_2(P_2O_7)_{0.99}$
C	0.91	36.4	0.47	44.6	0.11	19.1	$Ca_8(PO_4)_{4.15}(P_2O_7)_{0.95}$
D	0.95	38.0	0.63	59.9	≤0.01	≤1	$Ca_3(PO_4)_{1.99}$

[a] Calcium was titrated by using EDTA method. [b] Orthophosphate was assayed by the spectrophotometric method. [c] Pyrophosphate content was determined by vanadomolybdate spectrophotometric method, before hydrolysis of P–O–P bond in perchloric acid (6 M) at 100 °C for 1 h.

Depending on the solids, the percentage of ethanol was about 10 wt %. However, the precipitate prepared at 80 °C with a Ca/P ratio of 1.02 (sample **B**) included only 1 wt %.

The molar and mass compositions of calcium orthophosphate and pyrophosphate in solids heated to 700 °C for 10 h in a tubular furnace are reported in Table 4. According to the TGA curves in Figure 2, at this temperature, solids did not contain ethanol and the HPO_4^{2-} ions were condensed.[19,33] So, with the quantity of pyrophosphate ions formed during the heat treatment between 20 and 700 °C, the content of HPO_4^{2-} ions in the unheated solids was determined. The chemical determinations show that samples **A** and **B** contained only calcium and pyrophosphate ions but not orthophosphates. The formula found for these two compounds corresponds to calcium pyrophosphate (CPP) $Ca_2P_2O_7$. Now, the chemical formula of initial calcium phosphates **A** and **B** as prepared in ethanol was established, it was $CaHPO_4{\cdot}x$EtOH. During heating between 20 and 700 °C, the following reaction occurs:

$$CaHPO_4{\cdot}x\text{EtOH} \rightarrow x\text{EtOH}\uparrow + 0.5H_2O\uparrow + 0.5Ca_2P_2O_7$$

In sample **A**, the evaporation of ethanol and the dehydratation of HPO_4^{2-} ions occurred simultaneously from 200 °C. At the opposite, the dried precipitate **B** dissociated these two processes giving two separate weight losses.

Sample **D** heated to 700 °C contained only orthophosphates and not pyrophosphate ions. So, the chemical formula corresponds to tricalcium phosphate (TCP) $Ca_3(PO_4)_2$. Precipitate **D**, after drying, formed a solid with a Ca/P atomic ratio of 1.50 containing 15 wt.% of ethanol. This compound had the formula $Ca_9(PO_4)_6{\cdot}x$EtOH. When it is heated to 700 °C, the solvent is removed according to

$$Ca_9(PO_4)_6{\cdot}x\text{EtOH} \rightarrow x\text{EtOH}\uparrow + 3Ca_3(PO_4)_2$$

Solid **C**, heated to 700 °C, contained calcium and ortho- and pyrophosphate ions. Its composition corresponds to $Ca_8(PO_4)_4P_2O_7$. As pyrophosphate ions arised from condensation of the HPO_4^{2-} ions, it was possible to assign to the initial phosphate the formula $Ca_8(PO_4)_4(HPO_4)_2{\cdot}x$EtOH. During heating, the following reaction occurs:

$$Ca_8(PO_4)_4(HPO_4)_2{\cdot}x\text{EtOH} \rightarrow x\text{EtOH}\uparrow + H_2O\uparrow + Ca_8(PO_4)_4P_2O_7$$

Like sample **A**, solid **C** did not give two different weight losses on TGA for the removal of ethanol and condensation of hydrogenophosphate ions.

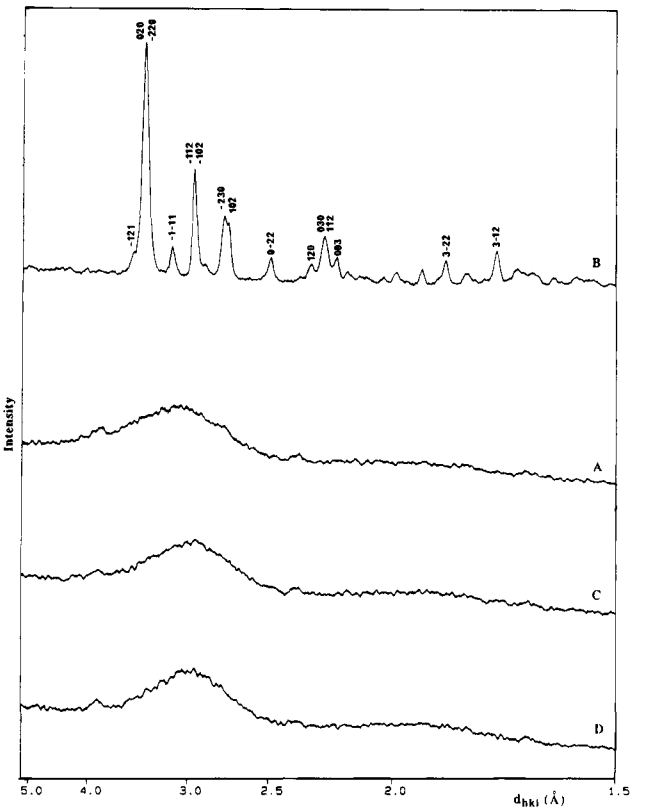

Figure 3. XRD patterns of the different calcium phosphates precipitated in ethanol and vacuum dried overnight for (**A**) amorphous $CaHPO_4$; (**B**) crystallized $CaHPO_4$ or monetite; (**C**) "$Ca_8(PO_4)_4(HPO_4)_2$"; (**D**) "$Ca_9(PO_4)_6$".

X-ray Diffraction. The XRD patterns of the four samples **A** (Ca/P = 1.00), **B** (1.00), **C** (1.33), and **D** (1.50) precipitated in ethanol and vacuum dried overnight are presented in Figure 3. Solid **B** prepared at 80 °C was crystallized and shows an XRD pattern identical with that of monetite $CaHPO_4$ (JSPDS 9-80). On the contrary, samples **A**, **C**, and **D** were completely amorphous with a characteristic halo whose maximum was located at about 3.0 Å. Nevertheless, there is slight difference in the position of the halo for the three amorphous samples. The maximun of the halo decreases from 3.06 Å for solid **A** to 2.94 Å for calcium phosphates **C** and **D**. As reported in Tables 3 and 4, samples **A** and **B** have the same formula $CaHPO_4$, but A precipitated at 5 °C was amorphous. So, the reaction temperature acts upon the crystallinity of the $CaHPO_4$.

Then, the different amorphous calcium phosphates were heated between 500 and 900 °C to understand their thermal behavior. After cooling rapidly to room

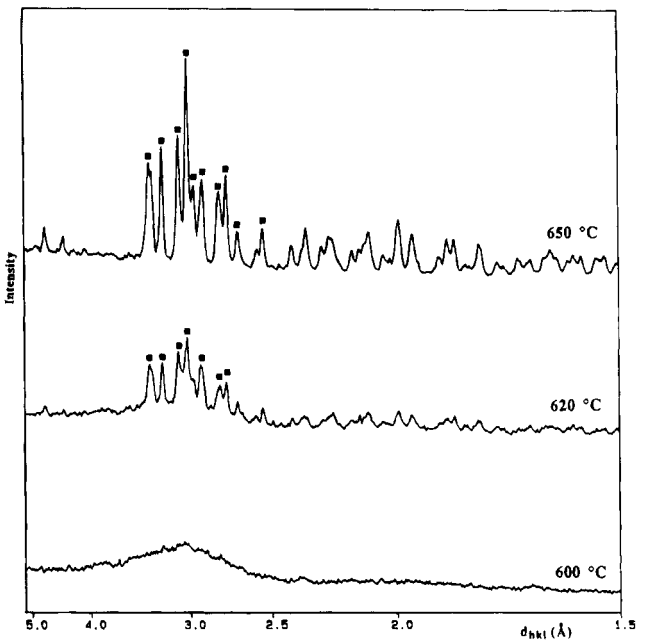

Figure 4. XRD patterns of sample **A**, amorphous "$CaHPO_4$" heated to different temperatures in helium for 10 h: (■) β-$Ca_2P_2O_7$.

temperature, they were studied by X-ray diffraction to determine the crystalline phases formed during the heat treatment.

In Figure 4, the XRD patterns of sample **A** heated at various temperatures are presented. Up to 600 °C, solid **A** remains amorphous. Sample **A** heated to 620 °C led to small broad reflections indicating the formation of a crystallized compound. At 650 °C, just before the exothermic peak observed by DTA, the XRD pattern shows a single phase for which the d_{hkl} positions and the intensities correspond to beta calcium pyrophosphate β-$Ca_2P_2O_7$ (JSPDS 9-346). It has been established that heating monetite $CaHPO_4$, between 450 to 718 °C, leads to γ-calcium pyrophosphate γ-$Ca_2P_2O_7$, and then this phase is transformed at 750 °C to β-$Ca_2P_2O_7$.[34-37] So, amorphous $CaHPO_4$ (sample **A**) shows a thermal behavior different from that of monetite. Solid **A** leads to metastable β-$Ca_2P_2O_7$ at 650 °C without the allotropic transformation from γ- to β-$Ca_2P_2O_7$.

In Figure 5, solid **C** (1.33) retains its amorphous character up to 600 °C. At 620 °C, small reflections through the amorphous halo are visible confirming the exothermic signal already observed with DTA. Forced crystallization is observed by further increasing the temperature. On the X-ray diffractogram at 700 °C, these rays are stronger and better separated. A mixture of two crystalline compounds, α-tricalcium phosphate α-$Ca_3(PO_4)_2$ (JSPDS 9-348) and β-$Ca_2P_2O_7$, can be identified. They are both metastable at these temperatures. On increasing the temperature, metastable α-TCP was converted progressively to β-TCP (JSPDS 9-169). At 900 °C, only a mixture of β-TCP and

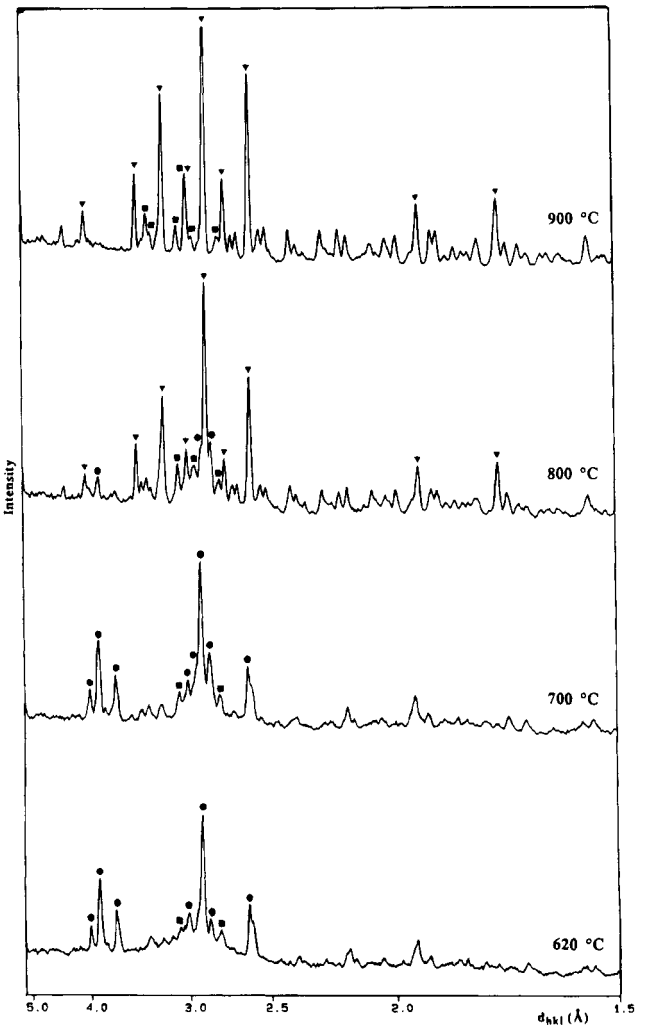

Figure 5. XRD patterns of sample **C**, amorphous "$Ca_8(PO_4)_4(HPO_4)_2$" heated at different temperatures in helium: (▼) β-$Ca_3(PO_4)_2$; (●) α-$Ca_3(PO_4)_2$; (■) β-$Ca_2P_2O_7$.

β-$Ca_2P_2O_7$ was observed. Nevertheless, it was not possible to make a quantitative evaluation of the relative amounts of each phase due to frequent superimpositions of the X-ray lines and to the lack of accurate calibration curves.

The thermal crystallization of amorphous sample **D** (1.51) is illustrated in Figure 6. The XRD patterns show that up to 550 °C, the solid remains noncrystalline. At 600 °C, the first phase to appear is β-TCP. However, around 700 °C, metastable α-TCP forms even though β-TCP is normally the stable phase up to 1150 °C. Then, on increasing temperature, α-TCP entirely converted to β-TCP. No other phases such as β-$Ca_2P_2O_7$ or hydroxyapatite (HAP) were detected by XRD. This is in aggreement with the Ca/P ratio of 1.51 determined by chemical analyses. The thermal crystallization of amorphous TCP precipited in aqueous reaction mixtures has been studied in previous papers.[38,39] The same thermal behavior is observed here with amorphous TCP prepared in anhydrous ethanol.

Infrared Spectroscopy. The infrared spectrum of solid **B**, prepared at 80 °C and with Ca/P atomic ratio close to 1.00, is shown in Figure 7. All IR frequencies

(34) Ranby, P. W.; Mash, D. H.; Henderson, S. T. *Br. J. Appl. Phys. Suppl.* **1955**, *4*, 18.
(35) McIntosh, A. O.; Jablonsky, W. L. *Anal. Chem.* **1956**, *28*, 1424.
(36) Parodi, J. A.; Hickok, R. L.; Segelken, W. L.; Cooper, J. R. *J. Electrochem. Soc.* **1965**, *112*, 688.
(37) Wikholm, N. W.; Beebe, R. A.; Kittelberger, J. S. *J. Phys. Chem.* **1975**, *79*, 853.
(38) Kanazawa, T., Umegaki, T.; Uchiyama N. *J. Chem. Tech. Biotechnol.* **1982**, *32*, 399.
(39) Eanes E. D. *Calcif. Tissue Res.* **1970**, *5*, 133.

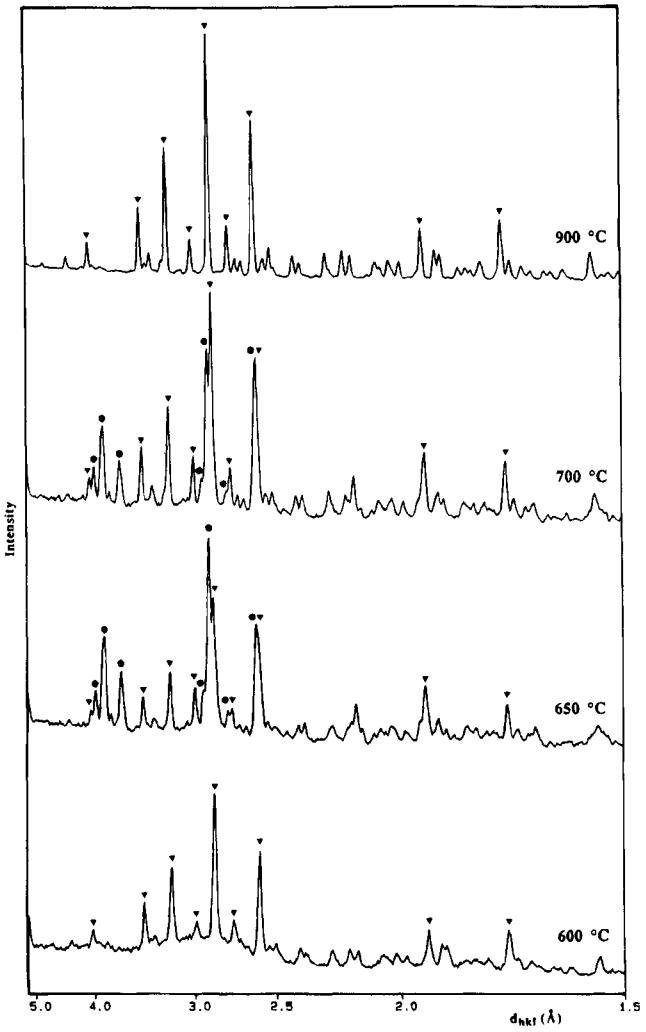

Figure 6. X-ray diffractograms of sample **D**, amorphous "$Ca_9(PO_4)_6$" heated to between 600 and 900 °C in helium: (▼) β-$Ca_3(PO_4)_2$; (●) α-$Ca_3(PO_4)_2$.

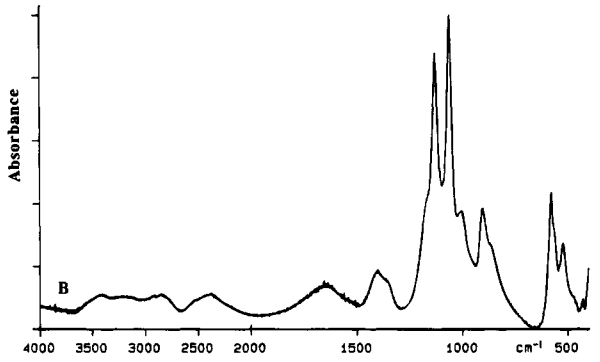

Figure 7. Infrared spectrum of anhydrous dicalcium phosphate prepared in ethanol at 80 °C with a $[Ca/P]_L$ of 1.00 (sample **B**).

are identical to the spectrum to monetite as described by Petrov and co-workers.[40]

The IR spectra of samples **A** (1.00), **C** (1.33), and **D** (1.50) are gathered in Figure 8. They present large bands, quite poorly defined but identifiable however by their frequencies. This confirms the amorphous state of these calcium phosphates. The large and strong band at 3400 cm^{-1} attributable to ν_{O-H} and shoulders at about

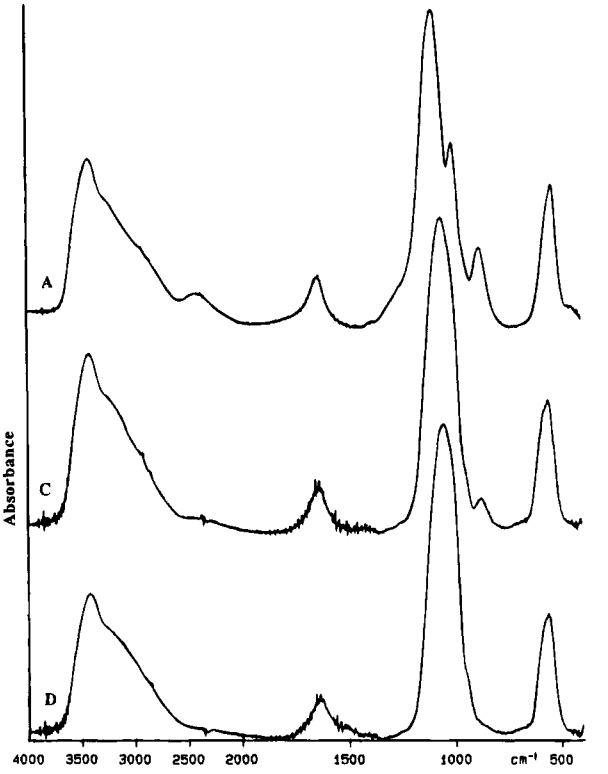

Figure 8. IR spectra of (**A**) amorphous $CaHPO_4$; (**C**) amorphous "$Ca_8(PO_4)_4(HPO_4)_2$"; (**D**) amorphous "$Ca_9(PO_4)_6$".

2800 cm^{-1} attributable to ν_{C-H} confirm the presence of ethanol adsorbed in these amorphous solids.

The attribution of bands situated near 450, 550, 950, and 1050 cm^{-1} corresponds respectively to the PO_4^{3-} ions vibration modes $\nu_2(E)$, $\nu_4(F_2)$, $\nu_1(A_1)$, and $\nu_3(F_2)$.[41]

Amorphous sample **A** precipitated at low temperatures produced an IR spectrum very different from crystallized sample **B** (monetite) prepared at 80 °C (Figure 7). Near 450 cm^{-1} (ν_2 mode), a shoulder with a weak intensity is observed. At 542 cm^{-1}, only one of the components of the ν_4 vibration appears. A band of an average intensity near 880 cm^{-1} corresponds to P–O(H) streching in HPO_4^{2-} groups. The spectrum shows strong and broad P–O vibrations at 1008 and 1094 cm^{-1}, attributable to ν_1 and ν_3 modes. On the other hand, this amorphous sample **A** did not produce IR bands at 1400 cm^{-1}, which were attibuted in crystalline monetite to hydrogen bridges between HPO_4^{2-} groups.[41] Near 2300 cm^{-1}, a large band of a weak intensity is also observed and corresponds to H–O(P) streching in HPO_4^{2-} ions.

Sample **C** (1.33) also has an IR spectrum with large PO_4^{3-} and HPO_4^{2-} bands that confirm its amorphous character. The ν_4 band at 560 cm^{-1} presents only one component. The elongation due to HPO_4^{2-} ions at 875 cm^{-1} are of much weaker intensity than that of sample **A**. The shoulder which corresponds to ν_1 mode is visible at 950 cm^{-1}. The strong vibration at 1061 cm^{-1} is assigned to the ν_4 mode.

The IR spectrum of sample **D** (1.50) is not very different from the former. Its IR bands are large confirming the amorphous state of this solid, evidenced also by XRD. It produces vibrations of tetrahedral

(40) Petrov, I.; Soptrajanov, B.; Fuson, N.; Lawson, J. R. *Spectrochim. Act.* **1967**, *23A*, 2637.

(41) Nakamoto, K. *Infrared spectra of Inorganic and Coordination compounds*; John Wiley and Sons: New York, 1963; p 197.

Table 5. Specific Surface Areas and Grain Sizes of Calcium Phosphate Samples Unheated and Calcined at 700 °C for 10 h in Helium

samples unheated	Ca/P; $T_{reaction}$ (molar; °C)	SSA[a] ($m^2\ g^{-1}$)	particle sizes[b] (nm)	samples heated to 700 °C	SSA[a] ($m^2\ g^{-1}$)	particle sizes[b] (μm)
A	1.00; 5	123	60–80	**A700**	10	1
B	1.00; 80	5	2000–5000			
C	1.34; 80	108	80–100	**C700**	11	3
D	1.52; 80	86	80–100	**D700**	8	5

[a] Specific surface areas (SSA) were measured by the single point BET method. [b] Particle sizes were determined by SEM.

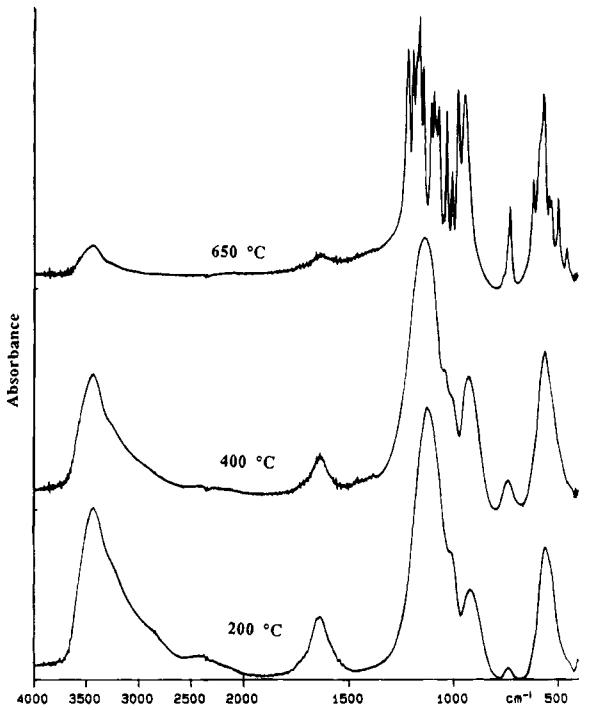

Figure 9. Infrared spectra of amorphous sample **A** heated to 200, 400, and 650 °C for 10 h in helium.

PO_4^{3-} ions: ν_4 located at 564 cm^{-1}, and ν_3 at 1051 cm^{-1}, as well as a shoulder at 950 cm^{-1} (ν_1). In the region 875–880 cm^{-1} there are no bands due to HPO_4^{2-} ions. This is in keeping with the chemical analysis of this solid heated to 700 °C (Table 4).

It is noticed that the position of the ν_4 vibration moves slightly toward the higher frequencies, whereas the position of the ν_3 band decreases, while the Ca/P ratio in the solids rises from 1.00 to 1.50. These slight differences in the IR spectra of the different amorphous solids confirm different local organization due to the various chemical compositions and local environments.

The IR spectra of amorphous sample **A** heated at 200, 400, and 650 °C are presented in Figure 9. The spectrum of the solid heated at 200 °C shows a new band at 730 cm^{-1} assigned to $P_2O_7^{4-}$ ions.[41,42] In heating to 400 °C, the intensity of this vibration increases while the large band at 2300 cm^{-1} attributed to $\nu_{H-O(P)}$ completely disappears. So, these spectra confirm that the dehydratation of HPO_4^{2-} into $P_2O_7^{4-}$ ions according to reaction 2 started at a very low temperature and is completed at 400 °C. On the other hand, these two spectra present large P–O bands, confirming the amorphous character of the heated solids already shown by XRD. Solid **A** remains amorphous until 650 °C, where IR frequencies are well-defined and are characteristic of β-$Ca_2P_2O_7$.[42] The desorption of ethanol with increasing temperature as observed by TGA was also confirmed by these spectra. It is clear that the intensity of the large band at 3400 cm^{-1} attributable to ν_{O-H} in EtOH decreases when the temperature of heating was raised. In the spectra of crystalline β-$Ca_2P_2O_7$, obtained by calcination of amorphous sample **A** at 650 °C, ethanol is totaly eliminated.

Specific Surface Areas and SEM Micrographs. Table 5 contains surface data measured by the BET method and grain sizes determined by SEM of the different calcium phosphates. The SEM micrographs in Figures 10–12 show spherical particles of several dozen nanometers in size for amorphous samples **A**, **C**, and **D** unheated. As a result of these very small particles, the noncrystalline solids have large specific surface areas ranging from 80 to 120 $m^2\ g^{-1}$. High surface energies effect a strong agglomeration which is clear in the electron micrographs. Indeed, in Figure 10, monetite (solid **B**) is crystallized into platelets of several microns. It therefore has a much smaller specific surface about 5 $m^2\ g^{-1}$.

Also, Figures 10–12 show the scanning electron micrographs of solids **A**, **C**, and **D** after heating in a helium atmosphere to 700 °C for 10 h. A strong grain growth owing to sintering of initial small particles by a diffusion process is observed in calcined samples. Joints and necks between initial spherical grains are easily visible. According to Table 5, specific surface areas of these heated solids show a marked decrease while the average particle dimensions increased due to the very active diffusion process. It is clear that the sintering process had already started at 700 °C resulting from crystallization in the amorphous samples evidenced also by DTA, XRD, and IR spectroscopy.

Discussion

The results show that it possible to prepare mineral calcium phosphates in ethanol. By simple variation of the experimental conditions at the start (Table 2), the precipitates obtained have the Ca/P atomic ratios expected (Table 3). When the ratio of reagents $Ca(OEt)_2$ and H_3PO_4 are varied from 1/1, 8/6, to 9/6 calcium phosphates of various chemical compositions are obtained following these reactions:

$$Ca(OEt)_2 + H_3PO_4 \rightarrow CaHPO_4\downarrow + 2EtOH$$

$$8Ca(OEt)_2 + 6H_3PO_4 \rightarrow Ca_8(HPO_4)_2(PO_4)_4\downarrow + 18EtOH$$

$$9Ca(OEt)_2 + 6H_3PO_4 \rightarrow Ca_9(PO_4)_6\downarrow + 18EtOH$$

This new synthesis route with these organic reagents allows the preparation of compounds with high purity

(42) Cornilsen, B. C.; Condrate, R. A. *J. Inorg. Nucl. Chem.* **1978**, *41*, 602.

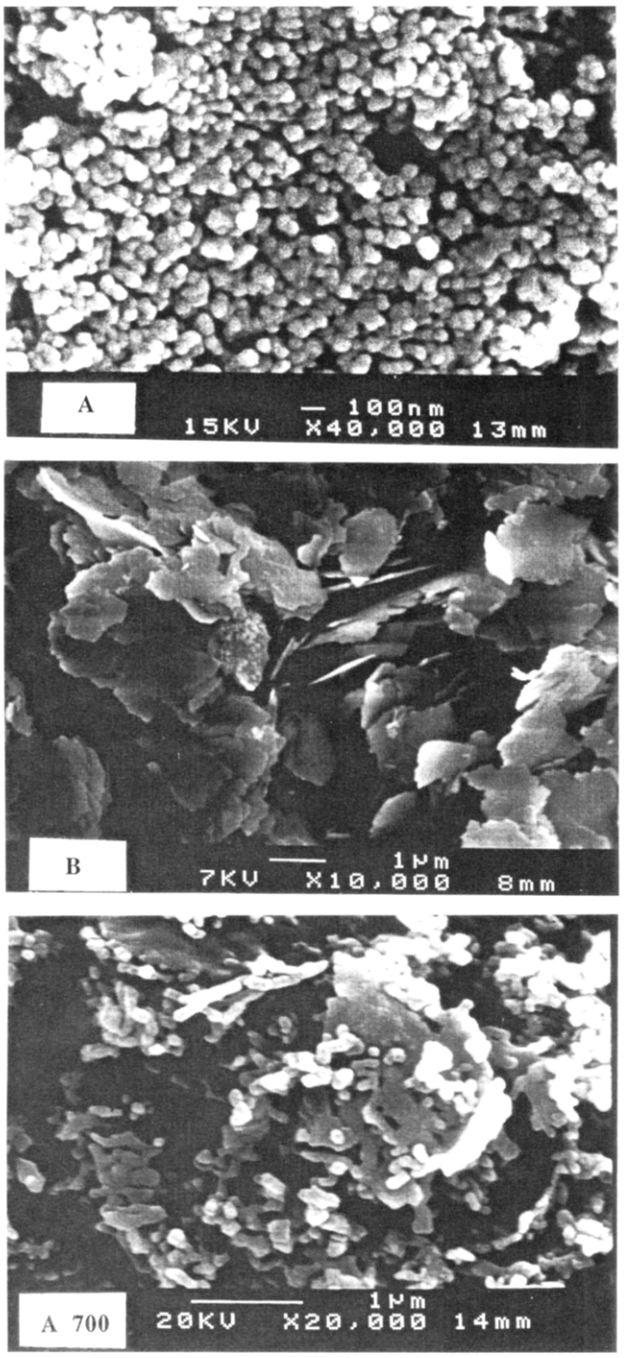

Figure 10. SEM micrographs of (**A**) amorphous $CaHPO_4$, (**B**) monetite, (**A700**) amorphous $CaHPO_4$ heated to 700 °C for 10 h in helium.

and enables their composition to be more accurately. The organometallic $Ca(OEt)_2$ has the advantage of being the calcium source and also of liberating the conjugate base of the solvent EtO^- into the medium. This strong base is necessary to neutralise the acidities of phosphoric acid and to precipitate the desired calcium phosphate. So, it is not necessary to add a mineral base, i.e., NH_4OH-, KOH-, or NaOH-like syntheses carried out in aqueous media. Another advantage is that the sole byproduct of the reaction is ethanol (solvent). Unlike precipitates obtained in water, these solids do not contain the contraions of the starting calcium and phosphate salts (Cl^-, NO_3^-, NH_4^+, K^+, etc.). The elimination of these ions, strongly attached to the precipitate by Coulomb attraction, often makes several rinses necessary. Thus, the calcium phosphates prepared from these reagents in ethanol are very pure and quantitatively obtained.

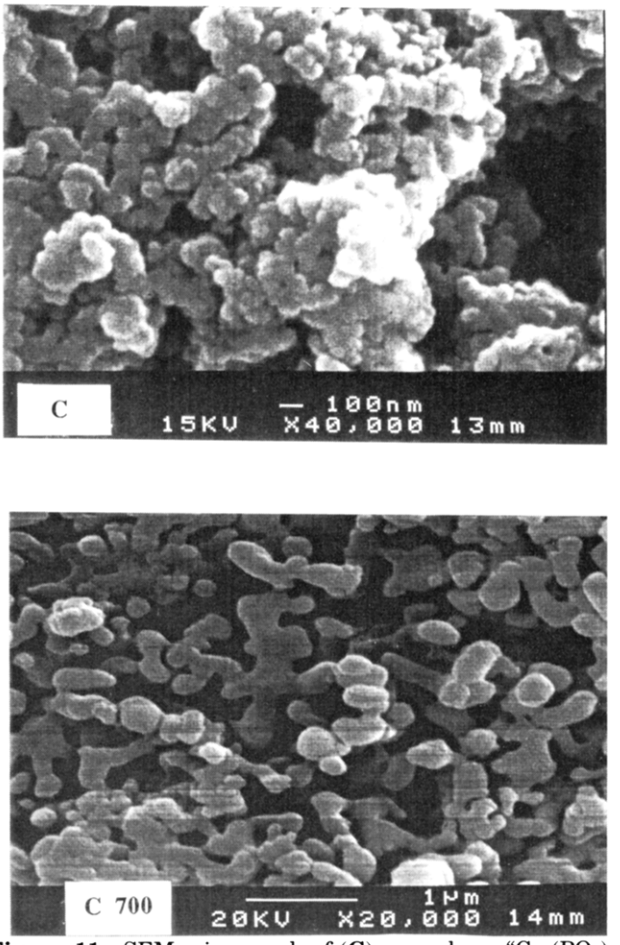

Figure 11. SEM micrograph of (**C**) amorphous "$Ca_8(PO_4)_4(HPO_4)_2$" and (**C700**) heated to 700 °C for 10 h in helium.

The use of ethanol in the precipitation of calcium phosphates leads amorphous solids with large surface energies and a high reactivity. In fact, the dielectric constant of ethanol at 25 °C ($\epsilon_{EtOH} = 24.3$) is much weaker than that of water ($\epsilon_w = 78.5$). Therefore, ethanol solvates ions in solution less well than does water.[43] The consequence of this is a strong decrease of the solubility of calcium phosphates or an increase in the rate precipitation. The first germs formed right at the beginning do not have the time to grow or to organize enough to form a crystalline network. The solids precipitated in this medium are amorphous and show a large delay in thermal crystallization (Figure 2) like compounds obtained by the sol−gel process, i.e., SiO_2, Al_2O_3, TiO_2.[44] Then, these amorphous precipitates thermically evolve into metastable calcium phosphates like β-$Ca_2P_2O_7$ or α-$Ca_3(PO_4)_2$. This thermal crystallization of initial amorphous samples around 700 °C into metastable phases confirm their high reactivity (Figure 4−6).

The high reactivity of these noncrystalline compounds can be seen in the temperature of condensation of HPO_4^{2-} ions. In fact, when dicalcium phosphate is crystallized into monetite, the dehydratation of HPO_4^{2-} groups occurs at 475 °C (Figure 1, curve B) to form

(43) Reichardt, C. *Effets de solvants en chimie organique*; Flammarion sciences: Paris, 1969; p 164.
(44) Brinker, C. J.; Scherrer, G. *Sol-Gel Science, The Physics and Chemistry of Sol-Gel* Processing; Academic Press: New York, 1990.

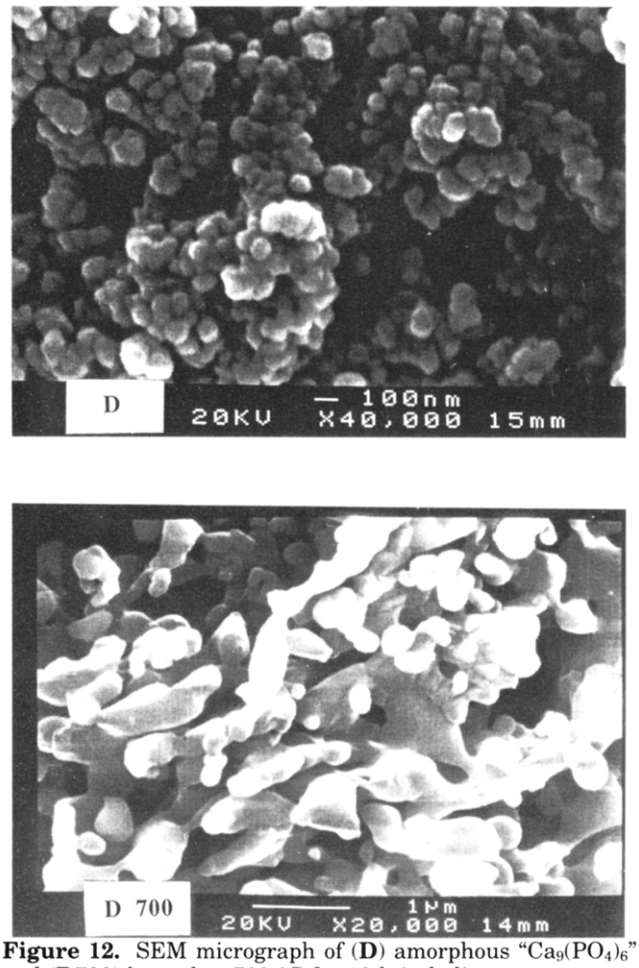

Figure 12. SEM micrograph of (**D**) amorphous "$Ca_9(PO_4)_6$" and (**D700**) heated to 700 °C for 10 h in helium.

γ-calcium pyrophosphate.[34-37] In amorphous sample **A**, precipitated at low temperature, this dehydratation started at 100 °C and finished at 400 °C (Figure 1, curve A, and Figure 9). Zahidi and co-workers have already etablished, by pyrophosphate chemical analysis and IR spectroscopy, that this dehydratation can occur earlier in amorphous calcium phosphates which contains HPO_4^{2-} ions (Ca/P = 1.33) prepared in a water−ethanol medium, than in crystalline precipitates.[19] A similar higher reactivity in the condensation of HPO_4^{2-} is observed here for amorphous calcium phosphates obtained in pure ethanol.

Also, this high reactivity can be observed in the diffusion process associated with their thermal crystallization. Several authors have shown that the sintering of HAP or TCP powders occurs only at 1100−1200 °C.[3,45] At these high temperatures, the particles can join by surface diffusion. The specific surface areas of these crystalline precipitates used in previous studies were considerably smaller (not exceeding 20 $m^2\ g^{-1}$) than those of finely divided amorphous calcium phosphates precipitated in ethanol (see Table 5). Because of this higher surface reactivity in our case, the sintering process starts at temperatures below 700 °C. TCP ceramics for biomaterial applications should be obtained at lower temperatures. It has been established that TCP ceramics present biocompatibility and bioresorption properties better than those of HAP ceramics.[3]

Physicochemical analyses have shown that noncrystalline calcium phosphates contain about 10% of adsorbed ethanol but only 1% when the solid is crystallized into monetite. According to TGA curves (Figure 1) and IR spectra of heated solids (Figure 9), ethanol is completely eliminated in the solids by 500 °C. It is well-known that amorphous TCP prepared in aqueous slurries retains 10−20 wt % of water which cannot be removed by drying at room temperature.[46] It has been proposed that adsorbed water stabilizes amorphous TCP. A similar conclusion can be invoked in the stabilization by ethanol of noncrystalline calcium phosphates.

Because they are nanosized, these calcium phosphates are difficult to study by the usual physicochemical analyses employed here. Nevertheless, there is slight differences in XRD patterns and IR spectra depending on the chemical composition. So, these solids show a short-range order. Certainly, it would be interesting to confirm these observations by techniques which are better adapted to the study of nanocrystals. More advanced techniques like radial distribution function (RDF) studies,[47] extended X-ray absorption fine structure (EXAF)[48] and solid-state NMR spectroscopy[49] have already been used in the case of amorphous TCP precipitated in water.

The ethanol-based synthesis of calcium phosphates by a soft chemistry process deserves to be enlarged to the preparation of compounds which cannot be precipitated in water, but only prepared in extreme conditions (solid−solid or solid−gas reactions at high temperatures or under high pressures). It is well-known that many cationic and anionic substitutions can occur in apatites.[4,5] This new route of synthesis in ethanol allows the preparation for example, of stoichiometric fluoro and chloroapatites (FAP, ClAP) which are difficult to synthesise in water (to be published).

Acknowledgment. We gratefully acknowledge Dr. J. Oquab for his technical assistance in SEM observations and Dr. E. Riviere for his helpful contribution in TG−DTA experiments.

(45) M. Jarcho; R. L. Salsbury; M. B. Thomas; R. H. Doremus *J. Mater. Sci.* **1979**, *14*, 142.

(46) Sedlak, J. M.; Beebe, R. A. *J. Colloid Interface Science* **1974**, *47*, 483.

(47) Grynpas, M. D.; Bonar, L. C.; Glimcher, M. J. *J. Mater. Sci.* **1984**, *19*, 723.

(48) Binsted, N.; Hasnain, S. S.; Hukins, D. W. L. *Biochem. Biophys. Res. Commun.* **1982**, *107*, 89.

(49) Tropp, J.; Blumenthal, N. C.; Waugh, J. S. *J. Am. Chem. Soc.* **1983**, *105*, 22.